

# Pattern Recognition Using Machine Learning Techniques

**Athmakuri Naveen Kumar**

Senior Software Engineer

**ABSTRACT:**

The technique of employing deep neural networks based on upgraded computer hardware has lately received interest in the field of pattern recognition research because of their greater accuracy compared to conventional approaches. In order to attain human-equivalent accuracy in picture classification, object identification, and segmentation, deep neural networks replicate the human visual system. The fundamental design of deep neural networks, which mimic human brain networks, is introduced in this chapter. Then, based on the bottom-up and top-down mechanisms, the most crucial aspects of the human visual perception process, we highlight the operational processes and applications of conditional generative adversarial networks, which are now under active investigation. Finally, new advancements in learning techniques for complex deep neural networks are discussed.

**PATTERN RECOGNITIONS OF HUMAN VISION:**

Hubel implanted microelectrodes in a cat under anesthesia's main visual brain in 1959. On the screen in front of the cat, they project various bright and dark patterns. They discovered that the "feature detector" that earned the Nobel Prize was what drove the neurons in the visual cortex. Each cell in the primary visual cortex, for instance, manages the most basic elements like lines, curves, and points when we recognise a human face. Target elements like eyes, brows, and noses are handled by the higher-level visual cortex via the ventral object identification pathway. The more complicated visual components are subsequently integrated with the context by the posterior inferior temporal cortex. The name of the anterior inferior temporal cortex (aITC), which more directly corresponds to a certain setting (such as whether the individual is male or female, residing in California, etc.), is more specific.

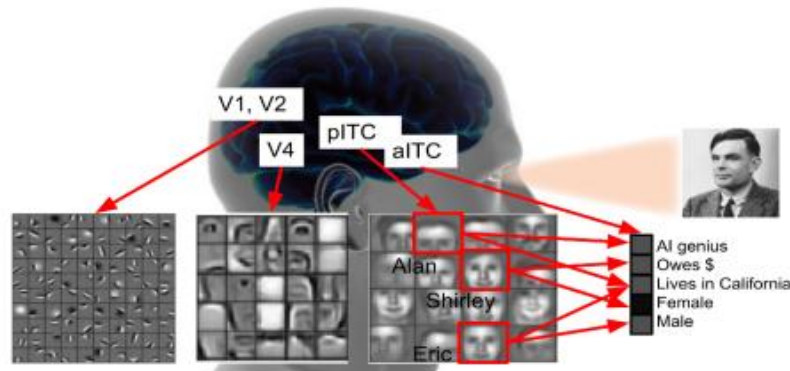


**Figure 1. Human visual system for Object recognition**

According to the preceding description, human visual perception has a hierarchical structure and is capable of massively parallel processing because to the hundreds of synaptic connections found in each neuron. Additionally, the winner-take-all architecture of human brain networks picks the most pertinent

neurons along the spatial dimensions in each layer. The three characteristics that motivated the development of artificial neural networks—hierarchical structure, parallel processing, and winner-take-all framework—recently advanced into deep convolutional neural networks. Max pooling and rectified linear units (ReLUs) are crucial parts of deep convolutional networks that may be built using a winner-take-all paradigm.

### **HUMAN VISION-INSPIRED CONDITIONAL GENERATIVE ADVERSARIAL NETWORKS:**

It is possible to think about object identification in human vision as a bottom-up process that combines lower level visual data in order to make sense of it. This technique can also be carried out top down, in the manner of visualising a new item based on semantic data (imagination). Conditional generative adversarial networks, a particular subclass of deep convolutional neural networks, may be conceptualised as an application of a human brain process that integrates bottom-up recognition (discriminator network) and top-down creativity (generator network). In addition to learning the generative model to minimise this loss, generative adversarial networks also learn the loss associated with distinguishing the produced output as real or fake. The conditional adversarial networks learn the loss function to train the mapping as well as the mapping function from the input to the output. The goal of the min-max game, which involves determining the minimum over  $g$ , or the parameters of our generator network  $G$ , and the maximum over  $d$ , or the parameters of our discriminator network  $D$ , is to be solved in order to train the generative adversarial networks.

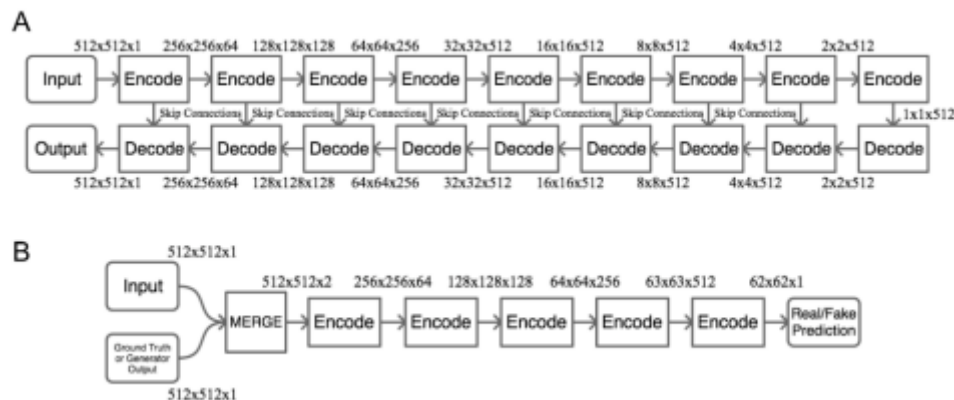
$$\min_{g} \max_{d} [E \log D(y) + E \log (1 - D(G(z)))]$$

The probability, or expectation, that the genuine data from the data distribution  $P_{data}$  are real is the first term in the objective function (1). The discriminator output for actual data  $y$  is the  $\log D(y)$ . In the event where  $y$  is genuine,  $D(y)$  is 1 and  $\log D(y)$  is 0, making the maximum possible. The second item in our generator network's equation is the expectation of  $z$  derived from  $P(z)$ , or the random data input (Figure 1). The result of our discriminator for the fabricated data  $G(z)$  is  $D(G(z))$ . The  $\log (1 - D(G(z)))$  gets extremely tiny (minimised) if  $G(z)$  is close to real,  $D(G(z))$  is close to 1, and so on.

### **PRECISION MULTI-BAND INFRARED IMAGE SEGMENTATION USING CONDITIONAL GENERATIVE ADVERSARIAL NETWORKS:**

It has been done to distinguish foreground and background classes in infrared pictures using generative adversarial networks. Losing two channels, leaving just one component channel to express pixel intensity in infrared pictures, is one of the main contrasts between infrared and conventional colour images. Because of this information loss, both the training and inference phases of feature extraction become more challenging. As an illustration, consider how the dynamic properties of the foreground and background intensities can alter depending on how much infrared light the thermal imager is able to record. Inconsistent characteristics are influenced by a variety of elements, including the amount of sunshine, reflected light, and the substance that makes up an item. It is more challenging to achieve accurate foreground-background segmentation since the object and background intensities in the pictures change across frames and wavelengths. It might be challenging for manual segmentation approaches to distinguish between ambiguous borders caused by high noise backgrounds with pixel intensities that are comparable to the object. The objects' poor contrast and low intensity characteristics at these infrared wavelengths also make proper categorization challenging. Particularly in contexts with noisy backgrounds, small features are places where precise segmentation is necessary for correct pixel

classifications. In order to handle the challenges of infrared picture segmentation, generative adversarial networks, which include a generator and discriminator, have proved to be a suitable fit. In comparison to other network models, generative adversarial networks are able to capture more significant characteristics because of the interaction between these structures. Image segmentation has employed digital image processing, filtering, and thresholding. However, when used on photos with uneven backgrounds, these techniques' segmentation accuracy diminishes. Adaptive thresholding has also been carried out using shallow neural networks. Even with a few hidden layers, a straightforward neural network would struggle to integrate complicated foreground and background information. While deep learning models can have up to 100 hidden layers, traditional neural networks only have one to three. Through a procedure known as feature extraction, DNN models often learn classification tasks from huge labelled datasets of pictures, texts, or audio. A DNN's multi-layered structure enables each layer to encode unique characteristics. Some layers can extract edge features while others may extract texture when categorising features in an image. The complexity of the encoded characteristics increases as the layers go closer to the output layer. The need for numerous training samples is one of the shortcomings of DNNs. Preparing training samples and ground truth data takes time. Occasionally, obtaining a large number of training examples is impossible. Utilising conditional generative adversarial networks, the DNN model under discussion learns a mapping from an input picture to an output image. Because generative adversarial networks are what they are, the model produces a loss function right from the training set. The exact segmentation boundary of the item is used as the ground truth in a collection of matched pictures, training conditional generative adversarial networks to learn mappings. The model is programmed to output a binary mask of the item from an input infrared picture of the object. The generator may create pictures that approximate the desired ground truths from the input image by using feedback from the discriminator.



Conditional generative adversarial networks for object segmentation are shown in Figure 2. By employing skip connections, the U-Net generator (A) produces output pictures based on input images while keeping structural similarity between the input and output images; (B) the discriminator (C) determines if the output of the generator is genuine or not.

With skip connections between each encoder and decoder layer, the generator design consists of a nine-layer encoder and nine-layer decoder. The encoder and decoder were both given an extra layer to boost the resolution from 256x256 to 512x512. The first encoder layer and the eighth decoder layer now have a skip connection added to them. To fit the input layer, an input picture is scaled into a 512x512 matrix. The input picture appears in the upper left corner of the first layer. The segmented map exits the generator's upper right side as data travels across the network. The network executes a 4x4 convolution,

batch normalisation, and a leaky rectified linear unit (LeakyReLU) activation function in each encoder layer. Each decoder layer in the network receives a 4x4 deconvolution, batch normalisation, and rectified linear unit (ReLU) activation function. To improve the segmentation accuracy of characteristics of certain objects that have been incorrectly identified, artificial training photos are employed. The target is pulled out, and the texture of the surrounding region is used to fill in the target's absence to provide a picture that only has the desired feature. The cropped feature is added on top of the background image after the item has been removed. During the model's retraining, enhancement photos are intended to improve the loss contribution of particular object attributes. By increasing the number of training images containing these emphasized loss contributions, the desired features are enhanced in the DNN.

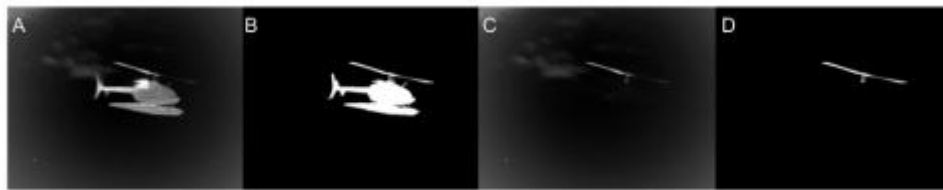
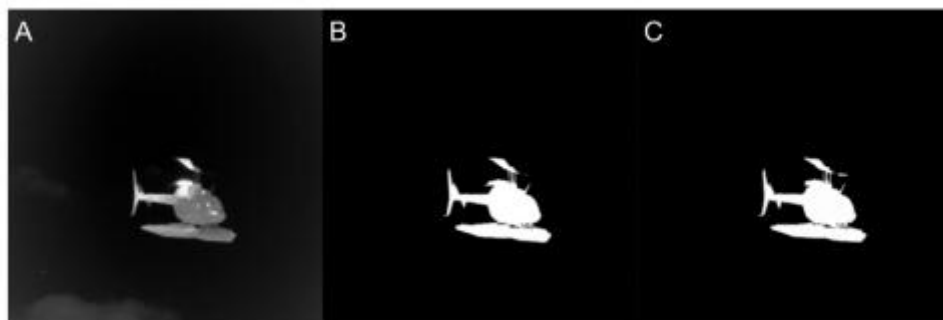


**Figure 3. Augmented FF Dataset, (A) Original image, (b) GT, and an example of an Augmented feature cropped Dataset: (c) missing rotor part, (d) GT of the missing rotor.**



**Retraining a DNN to improve features (Figure 4) The original picture, the first DNN output that omits the right side of the rotor blade, and the retrained DNN output that reconstructs the missing rotor blade component are shown in (a), (b), and (c), respectively.**

A semi-manual segmentation approach called GraphCut weights each zone according to how similar it is to neighbouring regions after dividing the entire frame into regions. Edges with low weights are divided into the foreground and the background. GraphCut requires a human selection of samples in the foreground and background to determine the class of its areas. To further fine-tune the segmentation, more manual sample choices may be added, but if there is a significant degree of similarity between some sections of the frame, incorrect categorization will still occur no matter how many human sample selections are provided. Applying an autonomously determined threshold will provide binary segmentation masks. The automated threshold for segmentation was carried out using iterative inter-means or IsoData. This technique uses a beginning threshold to distinguish between the foreground and background. The threshold is then adjusted by computing the average of two averages from the values of the pixels above and below the starting threshold. Until it exceeds the average of two averages from pixels above and lower than it, the original threshold is modified. By manually thresholding the picture, segmentation was carried out using ImageJ. Based on the precision of the segmented features and the volume of noise produced, the threshold value was chosen. A higher threshold tends to overlook low intensity elements like the antennas and rotor blades while removing the majority of the noise in the segmentation.

The segmentation of infrared images was carried out using a small-scale neural network. One input layer, one hidden layer, and one output layer made up this neural network. There were just 25 neurons in the hidden layer of this simple neural network. In comparison to the outdated GraphCut (19.0% XOR error) and thresholding approaches (10.3% XOR error), the basic neural network achieves respectable segmentation results (9.2% XOR error). The lack of generalisation across intensity variations in the foreground and background is a flaw in this small-scale neural network. A deep convolutional network implementation for semantic segmentation is DeepLab v2 (ResNet-101). Atrous convolution and atrous spatial pyramid pooling are employed in the specific method used here, without the usage of conditional random fields for post processing. When applying upsampled filters in the convolutional layers, atrous convolution refers to getting full resolution information. By using numerous filters with different sample rates, Atrous spatial pyramid pooling (ASPP) is employed throughout the feature abstraction phases to boost resistance against scale shifts. Figure 5 displayed the outcomes of the segmentation performed by DeepLab and the segmentation performed by JPL using modified conditional generative adversarial networks. Deeplab was able to recognise the object and distinguish it from its surroundings. The Deeplab model, however, was unable to accurately depict the object's border and was missing certain minor characteristics.

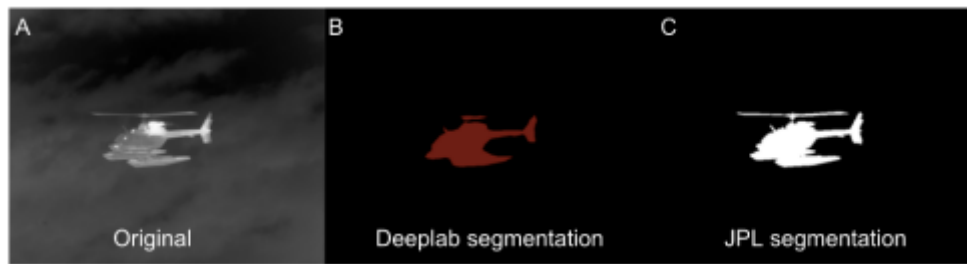


**Figure 5. Segmentation results: (A) Original image; (B) DeeplabResNet segmentation output; (C) JPL segmentation output using conditional generative adversarial networks.**

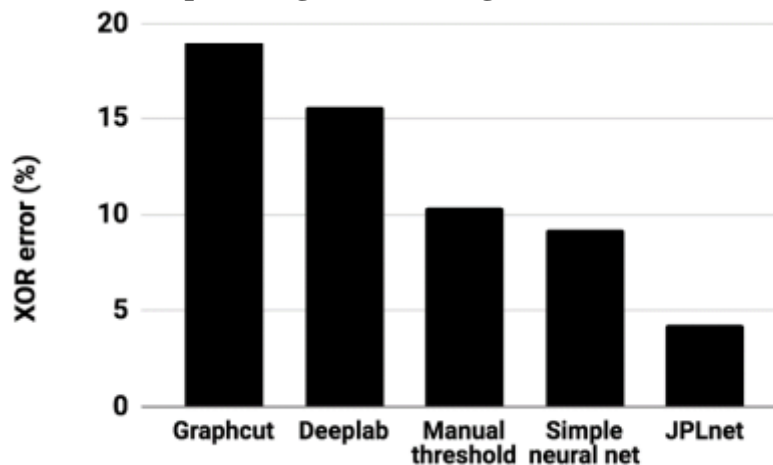


**Figure 6. Comparison of the segmentation results of Graphcut, Deeplab-ResNet, manual thresholding, simple neural network and JPL network**

In comparison to thresholding techniques, GraphCut, the DeepLab v2 model, and the simple neural network model, it has been demonstrated that the modified conditional generative adversarial networks model is capable of producing segmentation masks that are substantially more accurate. Even though the small neural network trained in less than a minute was able to average an XOR percentage of 9.2%, user input is still necessary. Both training and inference need manual selection of coordinates to draw a

bounding box around the object. The segmentation of small features near the low intensity regions is another challenge for the basic neural network. In infrared wavelength photographs, the conditional generative adversarial networks design has proven to be effective in precisely segmenting objects from a chaotic backdrop. The model successfully extracts low intensity features and gradient edges where techniques like iterative inter-means thresholding, manual thresholding, and GraphCut often fall short. Due to the conditional generative adversarial networks design, the DNN can be taught using a substantial amount of training pictures. In extremely busy backdrops, it showed evidence of reliable item detection, identification, and precision segmentation. Other DNN designs with a semantic segmentation focus can produce segmentation masks more effectively than thresholding techniques, but they frequently overlook important object properties.

**OCCLUDED OBJECT RECONSTRUCTION USING CONDITIONAL GENERATIVE ADVERSARIAL NETWORKS:**

Reconstructing partly occluded objects may be done using conditional generative adversarial networks. In order to support the future generation of first responders in carrying out safe, healthy, and effective missions, occluded object reconstruction can be helpful in providing situational awareness information. Each year while performing firefighting duties, more than 30,000 firefighters suffer injuries. Numerous firefighter injuries result from slips, trips, and falls, which highlights the demand for better ground assistance for firefighters. Occluded object reconstruction can give augmented reality glasses their "see-through" quality. Firefighters will be able to move through the event more safely and effectively if they can see through the fire. Additionally, firemen can locate patients who are partially hidden by items with speed. A sudden fire explosion (flashover phenomena) may be predicted by estimating the size and form of a fire in a partially obscured scenario. Firefighters can stay safe from hazardous settings and have a complete understanding of the situation if they are given the capacity to see through things. In this study, the scientists trained connections between distinct photos of flammable and dangerous objects and their partially occluded equivalents using generative adversarial networks. The whole architecture is shown in Figure 7, together with the generated output reconstruction pictures, input occluded photos, and ground truth images. The conditional generative adversarial networks can identify the association between the two images (original and occluded), transform or reconstruct the real input image into another image, whereas the original generative adversarial networks produce realistic-looking images from the random noise input z.

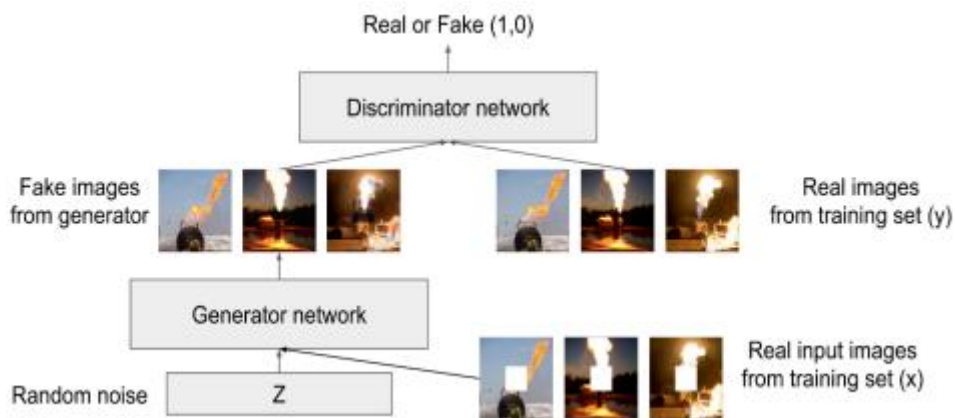


**Figure 7. Adversarial networks architecture.**

It might be useful to train the fundamental structure of the actual objects (fire, petrol tank, roof, etc.) and to retain the structural similarity of the input and output pictures because the objective was to rebuild partially obscured items in the image. As a result, the authors' generator was built on an encoder-decoder network that was gradually down- and up-scaled for effectiveness using U-Net architecture. The skip layer was then used by the network. The matching upsampling layer receives and is coupled to each downsampling layer, in other words. Finally, the downsampling layer might teach the upsampling layer crucial structural properties directly.(Figure 8) The authors gathered 100 photos from Google photos using the search terms "gas tank fire." They then utilised the photograph as input and applied synthetic occlusion to it. For training, we utilised 80 picture pairs that were randomly chosen, and for testing, we used 20 image pairs.

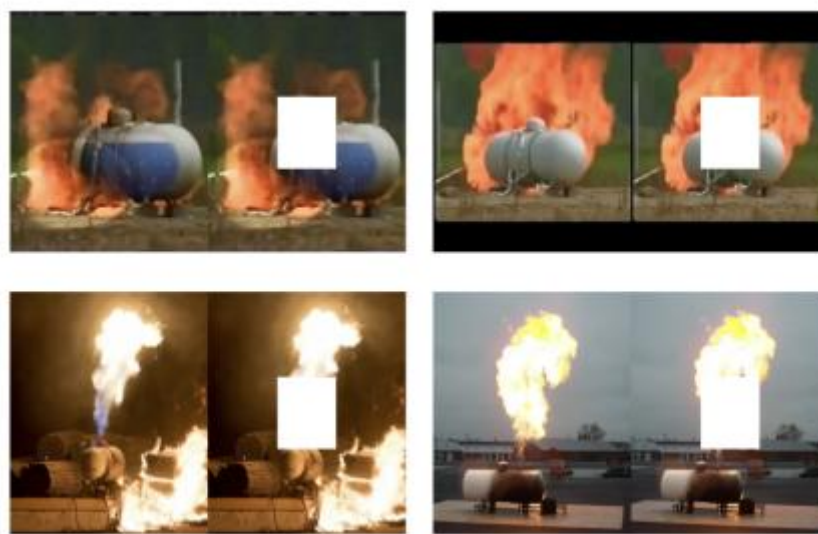


**Figure 8. Conditional generative adversarial networks - Representative training image pairs**

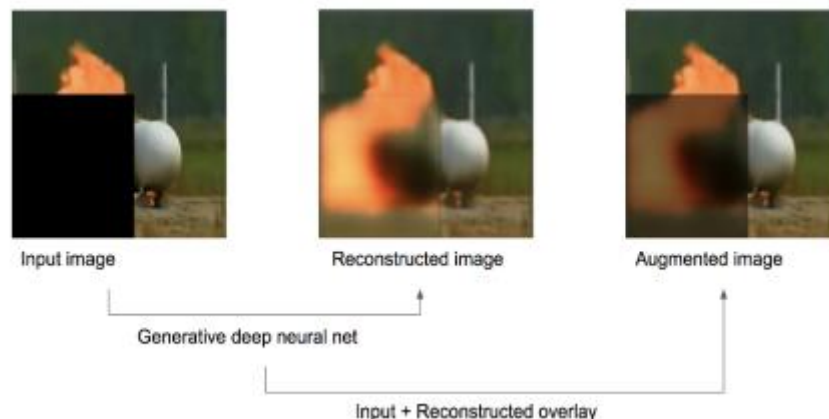


**Figure 9. Reconstructing a partially occluded object for first responders using conditional generative adversarial networks and augmented reality glasses**

The system recreated test pictures of partly obscured combustible items after conditioning conditional generative adversarial networks. The input picture was then overlapped with the reconstructed image to create "transparency" (Figure 9). Figure 10 presents representative reconstructions. According to Figure 10C, five out of the twenty test photos had inaccurate reconstructions (25% error rate). On tiny data sets (less than 100 samples), conditional generative adversarial networks have produced promising results. The speed of training is a benefit of tiny datasets. Less than five hours of training were used to get the

study's conclusions on a single NVIDIA GTX1080 GPU. This study may be utilised as a practical solution that includes greater understanding into the augmented reality glasses of the future generation of first responders because the conversion time for the test output image is less than 200 milliseconds. By solving mathematical models, occluded objects have been attempted to be reconstructed in augmented reality in earlier works. Compared to mathematical models, we were able to rebuild complicated backdrops and many objects more quickly using deep learning-based conditional generative adversarial networks. A nonlinear numerical model could be used to describe deep learning. In a challenging actual environment, mathematical models might not be reliable. One can argue that if the goal is to issue a warning and aid in victim identification in a fire emergency, we can do so without reconstructing the partially obscured item as we did in our case. It could be accurate, but by giving first responders a reconstruction of the obscured item, they can find other serious threats that a warning algorithm cannot spot. Additionally, lower level perceptual information (visualisation of occluded components) is more logical and quick than warning signals in terms of explaining and visible answers.

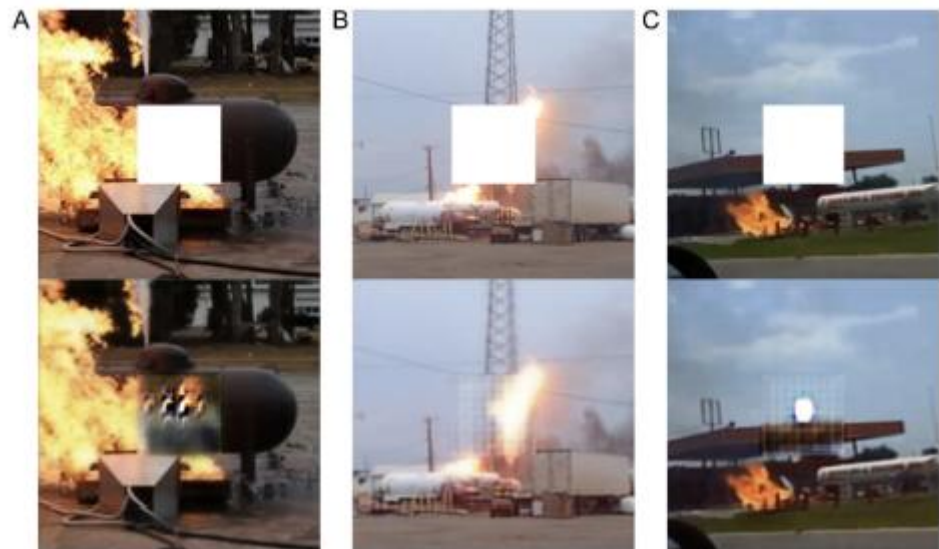


**Figure 10. Typical instances of a correct and faulty reconstruction. (A) An incorrect firing pattern was developed. (B) A precise firing pattern generation process was used. The gearbox tower that can be seen in the distance behind the fire was not rebuilt. (C) The development of a fake fire pattern is a bad example. The roof was appropriately created.**

There may not have been enough variation in the training data set, which is why certain test photos (Figure 4C) could not recreate the objects correctly. The amount and variety of training pictures should be enhanced as a further step to cope with different kinds of petrol tanks and fire incidents. Semantic reconstruction will be more accurate with the use of contextual information, such as building structure, fire origin, and gas/chemical sensor information. To improve accuracy, one may additionally include perspective shifts and image ageing.

### **IMAGE ENHANCEMENT FROM VISUAL TO INFRARED USING CONDITIONAL GENERATIVE ADVERSARIAL NETWORKS:**

To improve photos, conditional generative adversarial networks can be utilised. Firefighters can use contextual insights from deep learning-based image augmentation to anticipate flashover events. A fire that spreads across a gap fast due to the extreme heat is called a "flashover." The phenomenon that scares



firemen the most is flashover. To recognise, anticipate, and prepare for flashovers, firemen in particular need years of training and experience. Based on factors including fuel, temperature, and ventilation, previous investigations created mathematical models of flashover. In a prior research, the scientists used a numerical model to estimate the timing of flashover using oxygen concentration and mean flame surface size, and they were able to do so 70 seconds in advance. A technique to gauge a fire's temperature before to flashover was devised by another research. The structural information of the region and temperature/oxygen data from specific sensors are needed for these computational models of flashover fire, however they are impractical for use in actual fire mission applications. The colour, size, and form of the index of flashovers, which includes rollover (angel fingers), high heat, and dark smoke, may be measured. Hand-held thermal imaging cameras are used by firefighters to locate and assess the type of fire in low-light conditions. Hand-held cameras can only be operated with one hand, leaving the other hand free for other activities. The injury and death of a firefighter were caused by the improper use of a thermal imaging camera. Additionally, not all firemen presently have access to the infrared camera system because of the fire department's financial restrictions. We utilised a typical body camera and analysed the colour video stream to address this issue. To improve very dark fire and smoke patterns, we used generative adversarial neural networks. Then, we kept an eye on the fire and smoke's dynamic fluctuations. Finally, we discussed the potential occurrence dates for flashover. The fundamental concept derives from the fact that skilled firefighters can recognise fire and smoke quality visually even in extremely low light. Through a standard colour picture, they can visualise a thermal image. We thus used conditional adversarial network-based image-to-image conversion algorithms. The input picture is mapped to the output image by the network. Lewisville Fire Department and Texas State Fire Marshal's Office offered flashover training videos. These movies use the department's burn pod to demonstrate how a fire starts and develops through flashover at an early stage. Both a standard video camera view and a view from a thermal camera that firemen may see are shown in the film. This pilot investigation employed a total of 40 frames of regular and thermal picture pairings (30 photos for training, 10 images for the test). The amount of pixels in the red, green, and blue channels was determined by the authors. The average of the red and green channels is known as the yellow channel. According to the infrared camera's depiction of temperature, red is 300–500°F, yellow is 200–300°F, green is 100–200°F, and blue is 0–100°F. This illustrated the change in pixel count over time for each channel. Ten photos were utilised as inputs in the generative network test, from the start of the fire through the flashover transition (0-200 seconds). The final result was then produced (Figure 11). Early on in the blaze, modest smoke and the overall shape of the items (tables and couches) could be seen (Figure 11). The network was able to successfully produce hot smoke from the input picture, even in very dim settings (Figure 11B). A high heat was predicted in a flashover scenario, and the table item was still recognised (Figure 11C). By counting the pixels in each thermal component (red, yellow, green, and blue) in the output pictures, further analysis of the images was carried out (Figure 12). The scientists anticipated a flashover as early as 55 seconds before it really happened based on the temporal fluctuations of high temperature components (300–500°F and 200–300°F).

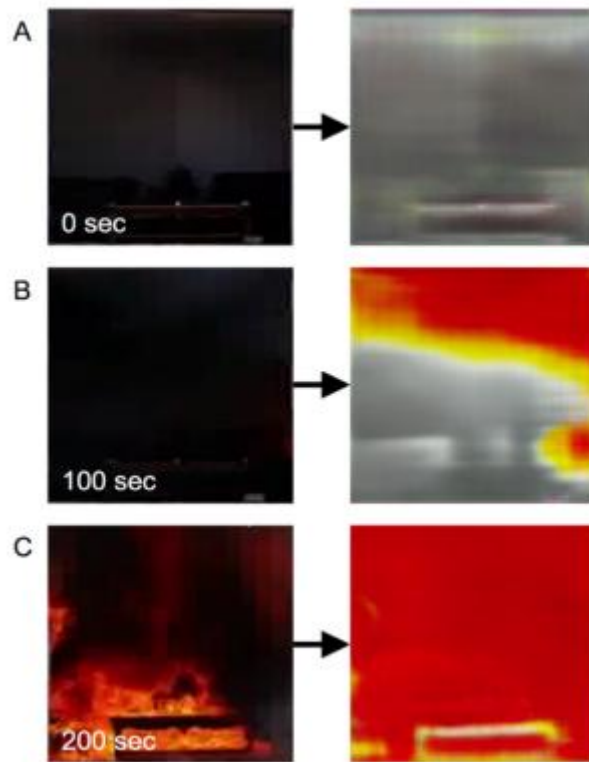


**Figure 11. Representative images of transformation from the visual to the thermal images using generative adversarial networks.**

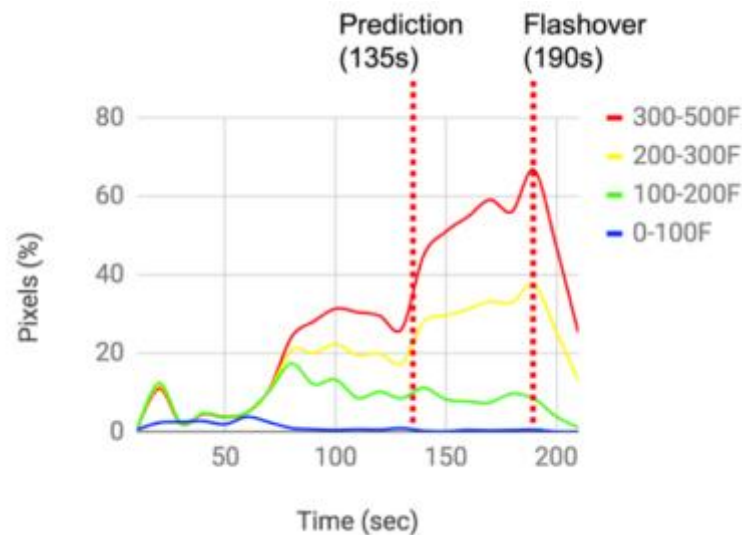


**Figure 12. Smoke and flame with Time and Pixels.**

The authors of this work demonstrated how standard body camera photos may be augmented and altered to reflect thermal information, and how this approach can be used to forecast flashover 55 seconds in advance. We visualised the modified intermediate outcomes in each latent space of the networks in order to completely comprehend the process of picture improvement from the ordinary visual image to the thermal image (Figure 13). Representative characteristics (such as fire and smoke) were improved in the early section of the space. Fire and smoke were further differentiated by the predicted temperature in the deeper half of the space. Then representative things (such as couches and tables) were found. Thermal data and realistic fire and smoke objects were therefore recreated in the final output picture. The internal

dynamics of the entire process, which is sometimes referred to as a "black box," may best be understood by visualising the hidden layers of neural networks. A thermal camera system built inside a firefighter helmet with an OLED display was demonstrated in a prior research. By automatically analysing thermal photos and measuring the temporal variations of the thermal content of smoke and fire, the authors' suggested technique may also be used to anticipate flashover. Regarding information overload, firefighters might get a lot of information without it being shown over the heat- or obscured-information on the screen. The firefighter's vision should be preserved as much as possible while yet getting the most crucial information.

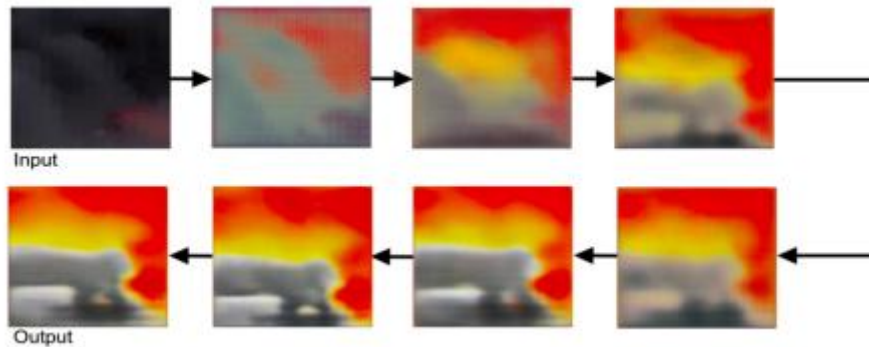


**Figure 13. Representative latent-space visualizations of the generative adversarial networks for image enhancement.**

**DATA AUGMENTATION FOR TRAINING DEEP NEURAL NETWORKS:**

Retrieving sufficiently large labelled training datasets, which can be costly and time-consuming to gather, is one of the main obstacles in deep learning. Using Deep Neural Network (DNN) models with a small number of initial labelled training samples is a novel method for training segmentation. In the process, artificial data is created, and then affine transformations are calculated to be applied to the artificial data via image registration. The technique starts with a tiny dataset and produces a high-quality synthetic dataset for augmented reality with significant volatility while preserving consistency with real situations. Results show an increase in average target confidence and better segmentation of various target attributes. Lack of readily available labelled data, which is advised in significant quantities for supervised deep learning, is the driving force behind the use of generated data. Data collection is challenging since it requires spending money and effort, especially for research teams with restricted resources. Deep learning is also prone to inefficient training, and completely training a deep neural network takes a lot of time, especially if there aren't enough computational resources. By advancing data accessibility and training optimisation, the rate of advancement in this discipline may be accelerated.



**Figure 14 shows an example of a synthetic video sequence for augmented reality that was produced by a series of transformations and picture superimpositions over backdrop frames.**

Data augmentation is a technique for expanding a dataset, and it has been shown to improve deep learning performance even using fake data. It has been demonstrated that data augmentation enhances

picture segmentation models, which is particularly advantageous when working with short training datasets. A dataset can be expanded by applying noise to a picture, conducting geometric adjustments, or modifying the original colours and contrast using a range of processing techniques. As a consequence, the enhanced dataset artfully offers fresh data that might enhance network generalisation and avoid overfitting. Synthetic data can offer useful extra training sets in circumstances when training data is difficult to gather and manually label. Synthetic targets are produced from templates for segmentation tasks and multiplied via the use of transformations. It is simple to binarize the resultant synthetic training targets using a global threshold to produce the matching labelled masks. This method is effective and reasonably priced for creating training samples and their labels. It might be argued that the amount and quality of the dataset are equally relevant to the optimisation of network parameters. The transformation matrices to be applied to the created data were retrieved from external films that show an item performing a desired motion. Only the dynamic characteristics of the item need to be representative; the videos don't have to all be in the same style. The sequence of frames can be placed onto a series of backdrop pictures once the synthetic data has been converted, as illustrated in Figure.

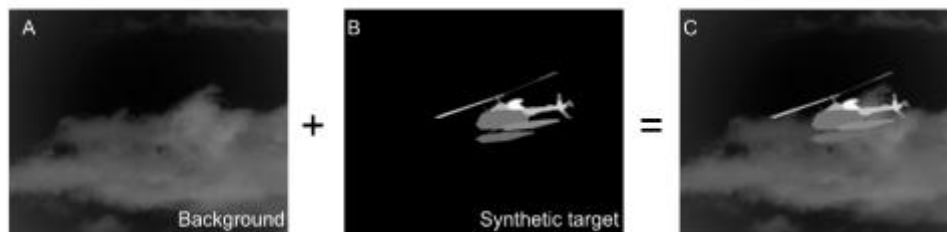


**Figure 15. Augmentation process: (a) Pre processed background frame, (b) Synthetic target frame, (c) Superposition of Target and background frames.**



**Figure 16. Example of progression of segmentations as more images are included**

**Table 1. Synthetic data training average test accuracy results on the 116-image test set and the 154-image test set**

synthetic training images	15	25	45	75	95	115
Segmentation accuracy	86.3%	92.86%	96.84%	94.1%	93.9%	90.2%

As the synthetic training samples are introduced to the training set, Figure 16 depicts the trend of increased accuracy. As more photographs are contributed, enhancements should continue to be made. Based on the results of the prior training, further training images are added to the training data set, however it is challenging to determine whether the additional images will be helpful to the particular problem set without testing after they have been propagated through the CNN. An initial set of artificial

target frames is part of the training set. To increase the training dataset, this collection of data is changed using the suggested technique. The test accuracy results are shown against the quantity of synthetic pictures introduced to the training set in Table 1. When more augmented synthetic photos are utilised to train the DNN, the DNN performs better. Because AR can automatically direct data augmentation by following the actual dynamics of an item in a reference movie, it is a suitable technique for generating data for DNN training. Modern AR has also enabled a wide range of simulation, educational, and medical applications. The usefulness of precision segmentation of infrared pictures has been proved by the outcomes of training a DNN employing AR for dataset augmentation. The idea of employing data augmentation to raise the calibre of training datasets is further supported by the fact that network performance improved as more photos were added to the datasets. Our AR technique scored an accuracy of 92.21% when utilising synthetic targets and 92.78% while using actual targets for single class, low-resolution infrared pictures. It also verifies the efficacy of training a DNN using synthetic data, since the 110 picture synthetic training dataset performed with accuracy within 1% of the 110 image real dataset. The findings imply that AR may be used as a practical method for teaching a DNN to segment infrared images precisely.

#### **INCREMENTAL TRAINING:**

Deep neural networks can benefit from incremental training because starting from scratch requires a lot of time and resources. Convolutional neural networks (CNN) have demonstrated its ability to deliver top-tier outcomes in a variety of fields, including speech recognition, natural language processing, and computer vision. Large volumes of training data are used by CNNs to increase generalisation and problem-set adaptation. CNNs can analyse raw data and develop pertinent features on their own, as opposed to earlier systems that need a large number of specialists to hand-engineer features. Only the design of the neural network is pre-defined; the CNN automatically extracts these features from the training data. These neural networks are good at adapting to new issues, but there are certain downsides. Deep neural networks have high computing requirements, require a lot of training data, and take a long time to fully train. It is challenging to choose and calibrate hyperparameters like learning rates, exponential decay rates, and loss function types. Training data sets must be separated into batches due to hardware constraints rather than propagating simultaneously across the network. Every time the network has to be trained with fresh data, the laborious procedure must be repeated from begin. By overcoming these problems, incremental training may be able to increase the CNN's accuracy to its maximum potential. One use of incremental training is to selectively improve a subset of missing characteristics without training on the complete data set. Incremental training can be used to concentrate on what was overlooked in earlier batches rather than providing new data and depending on random batching to update the new features. The advantages of training from scratch rise as the amount of training data remains essentially stable and becomes unusually big, whereas this incremental training strategy is best used during the fine-tuning stages of training with a small number of training samples. The conditional generative adversarial networks model was trained using an initial subset of 12 photos from 68 ground truths in an experiment, with the results presented in Figure 17. The first training on the 12 photos took 1.73 hours to complete to 1000 epochs. By including 8 new photos to the previously utilised 12-image set from the 68-image collection, a second training session was conducted. The weight matrix for the 20-image training session was chosen based on the epoch with the lowest L1 validation score from the 12-image training session. 1.96 hours were spent running this 20-image training session across 1000

epochs. The 20-image dataset was expanded with 16 more photos for the final training round, which followed the same procedure. In order to continue training for this new 36-image set, the lowest L1 validation scoring weight matrix from the 20-image set was employed. 1000 epochs of this 36-image training were completed in 2.9 hours. The whole collection of 68 pictures was used for the final training, which lasted an additional 4.05 hours and included 1000 epochs on top of the weight matrix from the 36-image set with the lowest L1 validation score. Results were more accurate when the training set was expanded incrementally and retrained using an earlier optimum weight matrix than when training was conducted as usual. An average XOR error percentage of 4.98% was obtained using the traditional method of training from scratch with the entire set of 68 images to 10,000 epochs for 42.45 hours, as opposed to 10.64 hours of training for a total of 4000 epochs and an average XOR error percentage of 4.23%. In contrast to training using a whole dataset with substantially longer running durations, this experiment demonstrates the usefulness of incremental training with new training pictures.

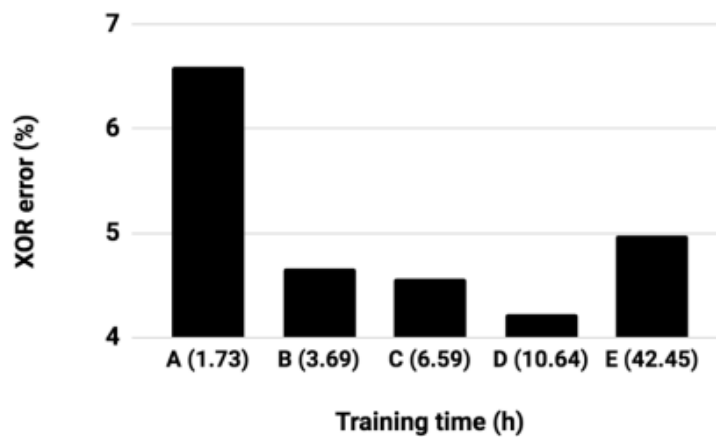


Figure 17. comparison of retraining process - performance

### CONCLUSION:

Deep neural networks, in particular conditional generative adversarial networks, have increased the accuracy of object identification and segmentation as well as picture categorization and improvement. In order to accurately segment and improve things, the system learns their structure and features, mimicking how humans learn about the laws of physics via experience. Incremental learning works well for training deep convolutional neural networks, much like it does for human learners. This technology will offer critical assistance that will let humans do any work more precisely and effectively.

### References:

1. Bhamare DP, Suryawanshi P. Review on Reliable Pattern Recognition with Machine Learning Techniques. *Fuzzy Information and Engineering*, 2018; 10(3): 362–377. <https://doi.org/10.1080/16168658.2019.1611030>.
2. Armengol E, Boixader D, Grimaldo, F. Special Issue on Pattern Recognition Techniques in Data Mining. *Pattern Recognition Letters*, 2017; 93: 1–2. <https://doi.org/10.1016/j.patrec.2017.02.014>
3. Kumar S, Gao X, Welch I. A machine learning based web spam filtering approach. In 2016 IEEE 30th International Conference on Advanced Information Networking and Applications (AINA), 2016.

4. Ermushev S, Balashov A. A Complex Machine Learning Technique for Ground Target Detection and Classification. *Int J Appl Eng Res.*, 2017; 11(1): 158–161.
5. Wu J, Yu Y, Huang C, Yu K. Deep multiple instance learning for image classification and auto-annotation. *Computer Vision and Pattern Recognition*, 2015. <https://doi.org/10.1109/cvpr.2015.7298968>.
6. Notton VG, Kalogirou S. Machine learning methods for solar radiation forecasting: a review. *Renew Energ.*, 2017; 105: 569–582.
7. Tajbakhsh N, Suzuki K. Comparing two classes of end-to-end machine-learning models in lung nodule detection and classification: MTANNs vs. CNNs. *Pattern Recognit.*, 2017; 63: 476–486.
8. Aginako N, Echegaray G, Martínez-Otzeta J. Iris matching by means of machine learning paradigms: a new approach to dissimilarity computation. *Pattern Recognit Lett.*, 2017; 91: 60–64.
9. Saii MM. Classification of Pattern Recognition Techniques Used Deep Learning and Machine Learning. *International Journal of Computer Science Trends and Technology (IJCSST)*, 2019; 7(3): 165-173.
10. Omarov B, Cho YI. Machine learning based pattern recognition and classification framework development. In *2017 17th International Conference on Control, Automation and Systems (ICCAS 2017)*. Ramada Plaza, Jeju, Korea, 2017.
11. Ushmani A. Machine Learning Pattern Matching. *International Journal of Computer Science Trends and Technology (IJCSST)*, 2019; 7(2): 4-7.
12. Chen S, Pande A, Mohapatra P. Sensor-assisted facial recognition: an enhanced biometric authentication system for smartphones. In *Proceedings of the 12th Annual International Conference on Mobile Systems, Applications, and Services*, 2014.
13. Yan Z, Zhan Y, Peng Z, Liao S, Shinagawa Y, Zhang S, Metaxas DN, Zhou X. Multi-Instance Deep Learning: Discover Discriminative Local Anatomies for Body part Recognition. *IEEE Transactions on Medical Imaging*, 2016; 35(5): 1332–1343. <https://doi.org/10.1109/tmi.2016.2524985>.
14. Monté-Rubio G, Falcón C, Pomarol-Clotet E. A comparison of various MRI feature types for characterizing whole brain anatomical differences using linear pattern recognition methods. *Neuro Image*, 2018; 178: 753-768.
15. Silasai O, Khowfa W. The Study on Using Biometric Authentication on Mobile Device. *NU. International Journal of Science*, 2020; 17(1): 90-110.
16. Findling R, Hölzl M, Mayrhofer RM. Mobile match-on-card authentication using offline-simplified models with gait and face biometrics. *IEEE Trans Mob Comput.*, 2018; 17(11): 2578-2590.
17. Nair HH, Amte GS, Todase NB, Dandekar PR. Face detection and recognition in smartphones. *International Journal of Advance Research and Development*, 2018; 3(4): 177-182.
18. Chen, L. C., Papandreou, G., Kokkinos, I., Murphy, K., and Yuille, A. L. “Deeplab: Semantic image segmentation with deep convolutional nets, atrous convolution, and fully connected crfs,” *IEEE transactions on pattern analysis and machine intelligence*, vol. 40, no. 4, pp. 834–848, 2018.
19. Yun, K., Lu, T., and Chow, E. “Occluded object reconstruction for first responders with augmented reality glasses using conditional generative adversarial networks,” in *Pattern Recognition and Tracking XXIX*, 2018, vol. 10649, p. 106490T.
20. Bowyer, M. E., Miles, V., Baldwin, T. N., and Hales, T. R. “Preventing deaths and injuries of fire fighters during training exercises,” 2016.